CHAPTER 128

ANALYSIS OF AIR-BUBBLE PLUMES

John D. Ditmars[1]
and
Klas Cederwall[2]

Abstract

Models are developed to describe the gross behavior of air-bubble plumes generated by point and line sources of air-bubbles released in stagnant water bodies of uniform density. The models predict plume width, velocities, and induced flow rates as a function of elevation above the source.

The analysis is confined to the plume mechanics and does not include the horizontal flow created at the surface by the plume. An integral similarity approach, similar to that used for single-phase buoyant plumes, is employed. Governing equations are found by applying conservation of mass, momentum, and buoyancy. The compressibility of the air and the differential velocity between the rising air bubbles and water are introduced in the buoyancy flux equation. Generalized solutions to the normalized governing equations are presented for both point and line sources of air-bubbles.

The results of the analyses are compared with existing large-scale experimental data. The comparisons indicate that the models predict the gross behavior of plumes well and yield estimates of the entrainment coefficients and lateral spreading ratios.

[1]Assistant Professor of Civil Engineering and Marine Studies, University of Delaware, Newark, Delaware, U.S.A.

[2]Assistant Professor, Division of Hydraulics, Chalmers University of Technology, Göteborg, Sweden.

Introduction

Air-bubble plumes have had a variety of applications in coastal waters including the inhibition of ice formation, pneumatic breakwaters, barriers to minimize salt water intrusion in locks, containment of oil spills, and mixing for water quality control. While air-bubble systems are often easily constructed and their application wide-spread, a description of their hydrodynamic performance is required. The details of such a two-phase flow are complex, but the gross hydrodynamic features of air-bubble plume are important for design purposes. The models developed here describe the gross behavior of air-bubble plumes generated by point and line sources of air-bubbles released in stagnant water bodies of uniform density. These models predict the plume width, velocities, and induced flow rates as a function of elevation above the source.

The discharge of air-bubbles into water creates a turbulent plume of an upward rising mixture of air and water by reducing the local bulk density of water. The rising plume entrains water from over the depth until it reaches the surface region, where as shown in Figure 1, a horizontal current is created. This study is restricted to the region below the influence of horizontal flow, and provides predictions of the flow delivered to this surface region. Experimental evidence indicates that the region of horizontal flow is approximately 0.25 of the water depth above a line source and somewhat less for a point source.

As air is discharged into water from a nozzle it breaks up into bubbles of discrete size. A study of the formation of gas bubbles in liquids has been reported by Davidson and Schüler (1). The rise and motion of individual gas bubbles in liquids have been investigated in many studies, and for example, Haberman and Morton (2), have reported on a comprehensive study on the rise velocity of single air bubbles in still water.

The similarity between the air-bubble plume and a single phase buoyant plume was first pointed out by Taylor (3) in a discussion of pneumatic breakwaters. He noted that the similarity existed only if the air bubbles were so small that their rise velocity relative to the induced plume velocity was negligible. The present study relaxes this restriction and attempts to account for the existence of such relative motion. Bulson (4,5) found semi-empirical relations for the maximum velocity and thickness of the layer of horizontal surface flow. Sjöberg (6) and Kobus (7) have investigated, both experimentally and analytically, air-bubble plumes using the concepts of jet and plume mixing.

Analysis and Model Development

The analysis of air-bubble plumes requires knowledge of the following system parameters:

q_o volume rate of air discharged at atmospheric pressure (volume rate/unit length for a line source)

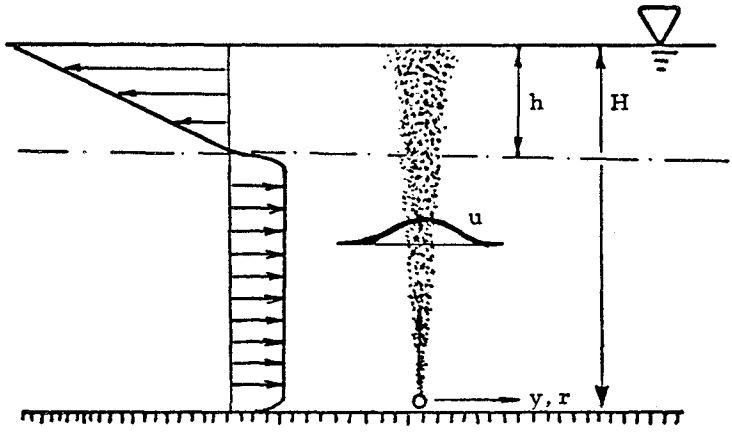

Velocity field close to the air-bubble plume.

Figure 1

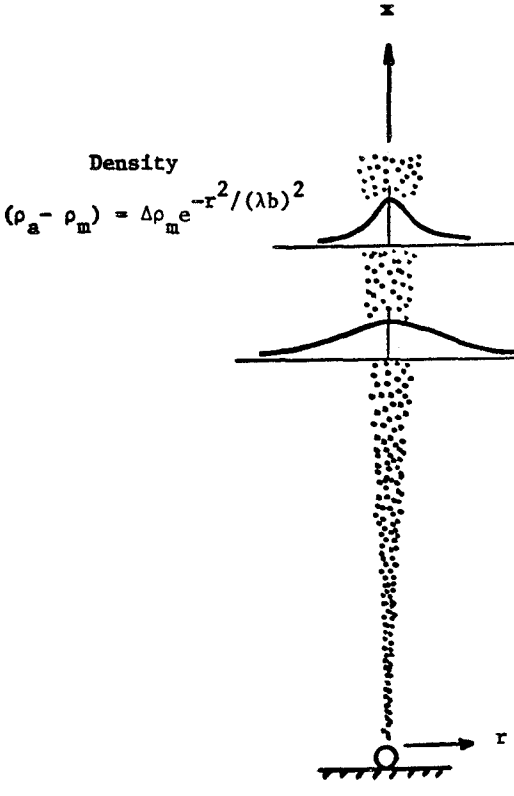

Figure 2

u_b velocity of the air bubbles relative to the gross plume velocity

H depth above the air source

H_o piezometric head equivalent of atmospheric pressure

It is assumed that for a first approximation u_b is equal to the terminal rise velocity of an air-bubble in a stagnant water environment and that the terminal value remains constant throughout the depth and is characteristic of all bubbles in the system. This approximation is reasonable, despite the fact that the bubbles probably vary in size in the plume, as u_b values for bubbles with diameters ranging from 10^{-3} to 10^{-2}m range only from about 0.2-0.3m/s (2). The expansion of the air bubbles as they rise through the water causes the driving force for the system, buoyancy, to vary and must be accounted for. This expansion is likely neither adiabatic nor truly isothermal but an intermediate process. The choice of expansion law does not significantly affect the results and the isothermal expansion is employed. Thus, if x is the vertical coordinate originating from the source (Figure 2) and q(x) is the local volume rate of air flow at x

$$q(x)\ (H_o + H - x) = q_o H_o \qquad (1)$$

and in particular at the source

$$q(o) = q_o\ \frac{H_o}{H_o + H} \qquad (2)$$

The air-bubble plume is analyzed following the similarity assumptions and integral techniques proposed by Morton et al. (8) for single-phase buoyant plumes. However, the effects of bubble "slip" relative to the plume motion and the changing buoyancy due to bubble expansion are included. The plume motion is assumed to be turbulent, and laterial profiles of plume velocity and density deficiency are assumed similar at all elevations and approximated by Gaussian distributions. The analyses for point and line sources are similar and the case of a point source is discussed in detail below.

A Point Source

As indicated in Figure 2, the velocity of the rising plume is given by

$$u(x,r) = u_m(x)\ e^{-r^2/b^2} \qquad (3)$$

where u is the local mean velocity and u_m is the centerline velocity for this axisymmetric case. The characteristic lateral dimensional of the plume is b(x) which is related to the standard deviation, σ, of the lateral velocity distribution by

$$\sigma = b/\sqrt{2} \tag{4}$$

The distribution of density deficiency between the plume and surrounding water is

$$(\rho_a - \rho_m) = \Delta\rho_m \, e^{-r^2/(\lambda b)^2} \tag{5}$$

where ρ_m is the local density of the air-water mixture and ρ_a the density of the ambient fluid. $\Delta\rho_m(x)$ is then the centerline density difference between ambient water and air-water mixture within the plume at a particular level. $1/\lambda^2$ is the turbulent Schmidt number and λ may be thought of as the ratio of lateral spread of density deficiency to momentum.

Following Morton et al. (8), the rate of entrainment of water into the plume is assumed to be directly proportional to the mean centerline velocity. The Boussinesq assumption that density differences may be neglected except in the buoyancy terms allows mass conservation in terms of volume flux. The volume at any elevation x is

$$Q = \int_0^\infty 2\pi \, u \, r \, dr = 2\pi u_m \int_0^\infty e^{-r^2/b^2} r \, dr = \pi u_m \, b^2 \tag{6}$$

The rate of entrainment, $\frac{dQ}{dx}$, is assumed to be

$$\frac{dQ}{dx} = 2\pi \, b \, \alpha \, u_m \tag{7}$$

where α is the coefficient of entrainment assumed constant.

Thus,
$$\frac{d}{dx}(u_m b^2) = 2 \, \alpha \, u_m \, b \tag{8}$$

The buoyancy flux of the air-water flow at any x is

$$B = \int_0^\infty 2\pi(u+u_b)(\rho_a-\rho_m) r \, dr = \pi u_m \Delta\rho_m \frac{\lambda^2 b^2}{1+\lambda^2} + \pi u_b \Delta\rho_m \lambda^2 b^2 \tag{9}$$

The buoyancy passes any level x with the velocity $(u + u_b)$, since it is due to the air bubbles which move relative to the plume. This formulation differs from that of Kobus (7) where the transport rate of buoyancy was determined from experimental data as a function of air discharge rate and bubble size. Equation (9) requires only knowledge of the bubble rise velocity relative to still water. The buoyancy flux at any level x is found using Eq. (1) to be

$$B = q_o(\rho_a - \rho_{air}) \frac{H_o}{H_o + H - x} \tag{10}$$

As $\rho_{air} << \rho_a$, B may be written

$$B = q_o \, \rho_a \, \frac{H_o}{H_o + H - x} \tag{11}$$

and hence the buoyancy flux relation is

$$\pi u_m \Delta\rho_m \frac{\lambda^2 b^2}{1+\lambda^2} + \pi u_b \Delta\rho_m \lambda^2 b^2 = q_o \rho_a \frac{H_o}{H_o + H - x} \quad . \tag{12}$$

Similarly, for the momentum flux with $\rho_m \approx \rho_a$ according to Boussinesq assumption

$$M = \int_0^\infty 2\pi u^2 \rho_a \, r \, dr = \frac{\pi u_m^2 \rho_a b^2}{2} \quad . \tag{13}$$

The driving force of the plume is the buoyancy, and the momentum flux equation is

$$\frac{dM}{dx} = \int_0^\infty 2\pi(\rho_a - \rho_m) g \, r \, dr = \pi g \, \Delta\rho_m \lambda^2 b^2 \tag{14}$$

which combined with Eq. (13) yields

$$\frac{d(u_m^2 b^2)}{dx} = 2g \frac{\Delta\rho_m}{\rho_a} \lambda^2 b^2 \quad . \tag{15}$$

Substitution of $\frac{\Delta\rho_m}{\rho_a}$ from Eq. (15) into Eq. (12) gives two equations to solve

$$\frac{d(u_m b^2)}{dx} = 2 \alpha u_m b \tag{16}$$

$$\frac{d(u_m^2 b^2)}{dx} = \frac{2 g q_o H_o}{\pi(H_o + H - x)\left(\frac{u_m}{1+\lambda^2} + u_b\right)} \quad . \tag{17}$$

Eqs. (16) and (17) must be solved to obtain the centerline values u_m and b as a function of x and $\Delta\rho_m$ can be found from Eq. (12). The discharge of water or the volume flux of the plume at any elevation can be found from Eq. (6).

Since a solution to the differential equations cannot be obtained in closed analytical form, a numerical integration has to be carried out. The numerical solution follows from a direct step-by-step integration of the equations

$$\frac{d u_m}{dx} = \frac{2 g q_o H_o}{\pi u_m b^2 (H_o + H - x)\left(\frac{u_m}{1+\lambda^2} + u_b\right)} - \frac{2\alpha u_m}{b} \tag{18}$$

$$\frac{db}{dx} = 2 \alpha - \frac{g q_o H_o}{\pi u_m^2 b (H_o + H - x)\left(\frac{u_m}{1+\lambda^2} + u_b\right)} \tag{19}$$

Near x = 0, $u_m >> u_b$ and hence Eqs. (18) and (19) take the following form

$$\frac{du_m}{dx} = \frac{2\ g\ q_o H_o (1+\lambda^2)}{\pi u_m^2 b^2 (H_o+H-x)} - \frac{2\alpha u_m}{b} \tag{20}$$

$$\frac{db}{dx} = 2\ \alpha - \frac{g\ q_o H (1+\lambda^2)}{\pi u_m^3 b (H_o+H-x)} \tag{21}$$

These are the governing equations for a simple plume due to a source of buoyancy only, and their closed form solution provides the starting conditions for the numerical integration

$$b = \frac{6}{5}\ \alpha\ x \tag{22}$$

$$u_m = \left[\frac{25\ g\ q_o H_o (1+\lambda^2)}{24\ \alpha^2\ \pi (H_o+H)}\right]^{1/3} x^{-1/3} \tag{23}$$

where x = 0 corresponds to the "mathematical origin." This "mathematical" or "virtual" source, as in single phase-plume analyses, is usually located below the real source of finite dimension.

A Line Source

The analysis of a two-dimensional air-bubble plume from a line source (which may be generated by a row of closely spaced orifices) is similar to that for the point source. For a lateral coordinate y, the velocity and density deficiency similarity profiles are given by

$$u(x,y) = u_m(x)\ e^{-y^2/b^2} \tag{24}$$

$$(\rho_a - \rho_m) = \Delta\rho_m\ e^{-y^2/(\lambda b)^2} \tag{25}$$

respectively.

The air discharge, q_o, has units of volume flux/unit length of source for this case and the volume flux/unit length at any elevation in the plume is

$$Q = \int_{-\infty}^{\infty} u\,dy = \sqrt{\pi}\ u_m b \tag{26}$$

The integral forms of the conservation of mass, buoyancy, and momentum, applied as for the point source case, yield the governing equations,

$$\frac{d}{dx}(u_m b) = \frac{2}{\sqrt{\pi}} \alpha u_m \tag{27}$$

$$\frac{d}{dx}(u^2_m b) = \frac{\sqrt{2}\, g\, q_o\, H_o}{\sqrt{\pi}(H_o+H-x)\left[\frac{u_m}{\sqrt{1+\lambda^2}} + u_b\right]} \cdot \tag{28}$$

Reduced for quadrature these are

$$\frac{du_m}{dx} = -\frac{2\,\alpha\, u_m}{\sqrt{\pi}\, b} + \frac{\sqrt{2}\, g\, q_o\, H_o}{\sqrt{\pi}\left[\frac{u_m}{(1+\lambda^2)^{1/2}} + u_b\right](H_o+H-x)u_m\, b} \tag{29}$$

$$\frac{db}{dx} = \frac{4\alpha}{\sqrt{\pi}} - \frac{\sqrt{2}}{\sqrt{\pi}} \frac{g\, q_o\, H_o}{\left[\frac{u_m}{(1+\lambda^2)^{1/2}} + u_b\right](H_o+H-x)\, u^2_m} \cdot \tag{30}$$

As for the point source case, near $x = 0$, $u_m >> u_b$, and the equations reduce to the simple two-dimensional plume equations which have the following solutions which provide the starting conditions for the numerical integration of Eqs. (29) and (30),

$$u_m = \left[\frac{g\, q_o H_o \sqrt{1+\lambda^2}}{\sqrt{2}\,\alpha(H_o+H)}\right]^{1/3} \tag{31}$$

$$b = \frac{2}{\sqrt{\pi}} \alpha\, x \cdot \tag{32}$$

Generalized Solutions to the Governing Equations

The governing equations for both the point and line source cases considered above require numerical integration to determine the centerline velocity, u_m, and the characteristic lateral dimension, b, and thus the plume width and volume flux at any elevation x. The governing equations and starting conditions for both cases were normalized using the system parameters to yield equations in terms of a dimensionless square root of the momentum flux, v, and a dimensionless mass flux, w, as shown in Table 1. The two governing independent parameters for each case G, a source parameter, and P, a scaling parameter for the water depth, are defined in Table 1.

Solutions of numerical integration of the normalized equations for a range G values of practical interest for a point source are given in Figure 3. Figure 3a shows the variation of the dimensionless centerline velocity v^2/w with dimensionless height above the source z, where

Air-Bubble Plumes in Homogeneous Environment

Case	Normalized Differential Eqs.	Starting Conditions	Parameters and Boundary Conditions
General Case, Point Source	$\frac{dw}{dz} = -2Gv$ $\frac{dv}{dz} = \frac{w}{z(v^3 + wv)}$	$w=\frac{6}{5}\left(\frac{9}{5}\right)^{\frac{1}{3}} G^{4/3}(1-z)^{5/3}$ $v = \left(\frac{9}{5}\right)^{\frac{1}{3}} G^{1/3}(1-z)^{2/3}$ $v^2 > w$	$G=\pi^{\frac{1}{2}} \frac{(H_o+H)\,\alpha\,(1+\lambda^2)\,u_b^{3/2}}{(g\,q_o\,H_o)^{\frac{1}{2}}}$ $z = 1$ to $z = P = H_o/(H_o+H)$
General Case, Line Source	$\frac{dw}{dz} = -G\frac{v}{w}$ $\frac{dv}{dz} = -\frac{w}{z(v+w)}$	$w=2^{1/6} G^{2/3}(1-z)$ $v=2^{1/3} G^{1/3}(1-z)$ $v > w;\ G < \sqrt{2}$	$G=2^{\frac{1}{2}} \frac{(H_o+H)\,\alpha\,(1+\lambda^2)\,u_b^3}{g\,q_o\,H_o}$ $z = 1$ to $z = P = H_o/(H_o+H)$

Table 1

Figure 3

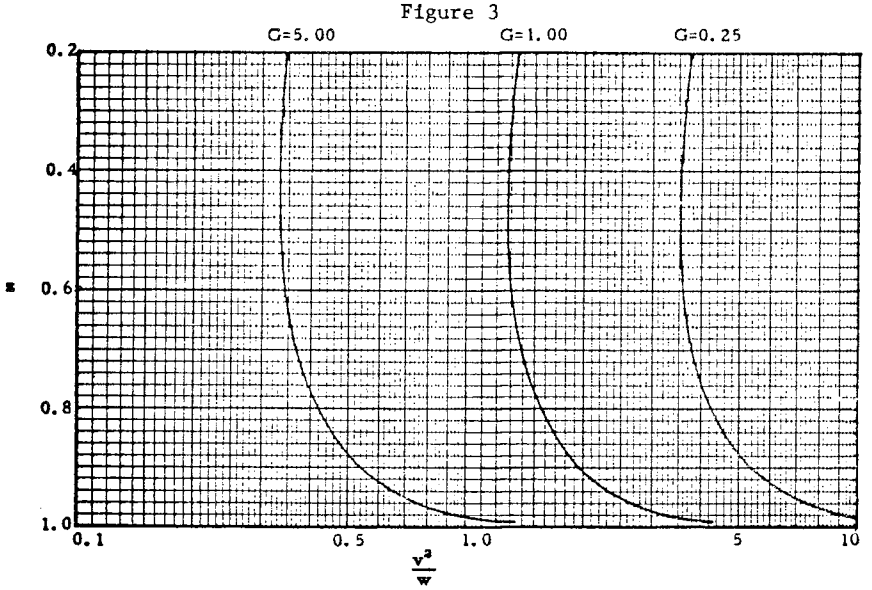

(a) **General solution of the three-dimensional air-bubble plume for G equal 0.25, 1.0 and 5.00. The centerline velocity** $u_m = (1+\lambda^2)u_b \frac{v^2}{w}$.

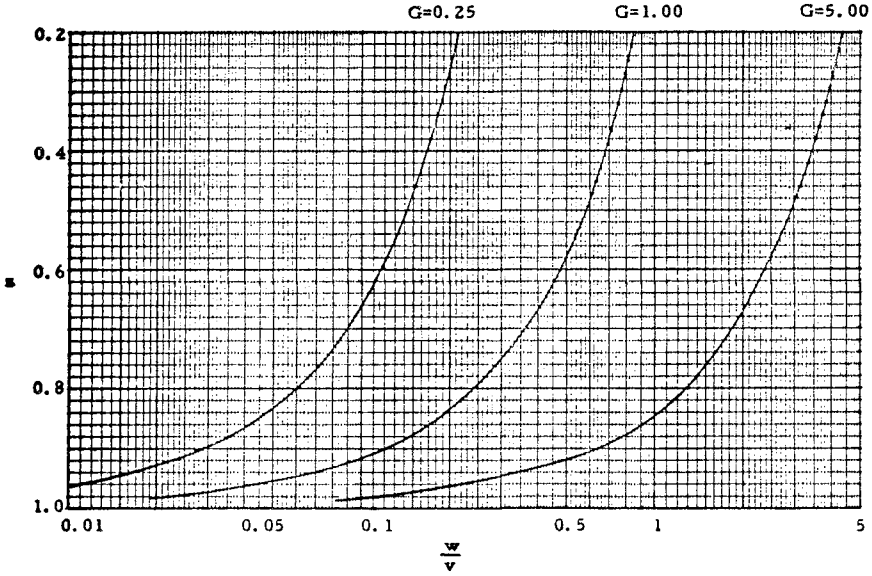

(b) **General solution of the three-dimensional air-bubble plume for G equal 0.25, 1.00 and 5.00. The nominal half-width** $b = \left[\frac{g q_o H_o}{\pi}\right]^{\frac{1}{2}} (1+\lambda^2)^{-1} u_b^{-3/2} \frac{w}{v}$.

$$z = \frac{H_o + H - x}{H_o + H} \tag{33}$$

and

$$u_m = (1+\lambda^2) u_b \frac{v^2}{w} \cdot \tag{34}$$

Figure 3b shows the variation of the dimensionless lateral dimension w/v with z, where

$$b = \left| \frac{g\, q_o H_o}{\pi} \right|^{\frac{1}{2}} (1+\lambda^2)^{-1} u_b^{-3/2} \frac{w}{v} \cdot \tag{35}$$

Similar solution curves are given in Figure 4 for a line source of air bubbles. Figures 4a and 4b show the variation of the dimensionless velocity, v/w, and the dimensionless lateral dimension, w^2/v, with depth, z, respectively. For the line source, the dimensional parameters are found from

$$u_m = (1+\lambda^2)^{\frac{1}{2}} u_b \frac{v}{w} \tag{36}$$

and

$$b = \frac{\sqrt{2}\, g\, q_o H_o}{\sqrt{\pi}(1+\lambda^2) u_b^3} \frac{w^2}{v} \cdot \tag{37}$$

The application of these generalized results requires, in addition to the system characteristics, determination of appropriate values of the entrainment coefficient, α, and the spreading ratio coefficient, λ, for both point and line air-bubble sources. Also, the location of the "virtual" source below the real source must be determined. Application of the plume models to experimental data was undertaken for verification of the model predictions and determination of these mixing parameters.

Comparison With Experimental Data

Large-scale laboratory experiments with both point and line source air-bubble plumes have been reported by Kobus (7). The point sources were located in 4.5m of water and consisted of orifices ranging from 0.05 cm to 0.5 cm in diameter with an air discharge range of 130 cm^3/s to 6200 cm^3/sec. The line sources were located in 2m and 4.3m of water and consisted of 0.1 cm diameter orifices spaced 10 cm apart with an air discharge range of 3000 cm^3/s-m to 10,000 cm^3/s-m. Kobus measured velocity profiles in the plumes with a current meter and reported these results for a variety of air discharges. The lateral velocity profiles indicated that the Gaussian profiles assumed in the analyses were a good approximation to the data.

The models developed above for point and line air-bubble plumes were applied to the experimental systems reported by Kobus (7), and predictions of centerline velocity and lateral spreading were made for a range of values of the entrainment coefficient and the lateral spreading ratio to determine best fits to the data (9). The location for the virtual source was found to be 0.8m below the real source for

Figure 4

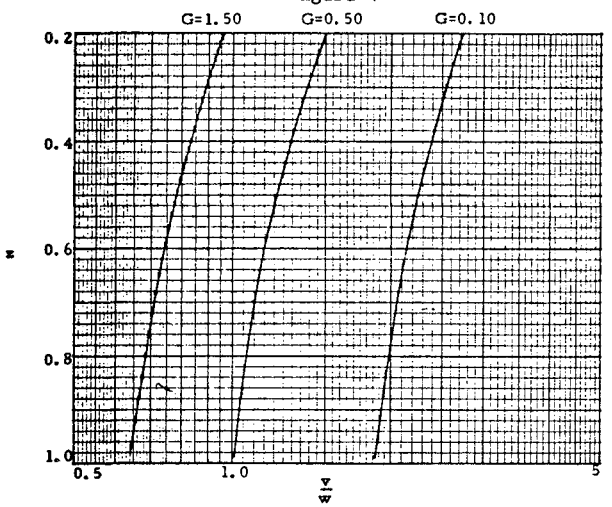

(a) General solution of the two-dimensional air-bubble plume for G equal 0.10, 0.50 and 1.50. The centerline velocity $u_m = (1+\lambda^2)^{\frac{1}{2}} u_b \frac{v}{w}$.

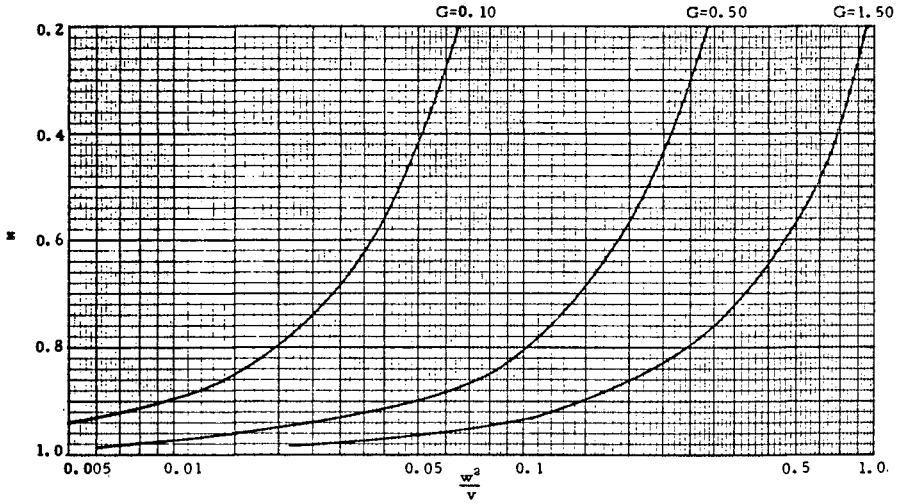

(b) General solution of the two-dimensional air-bubble plume for G equal 0.1, 0.5 and 1.5.

The nominal half-width $b = \frac{\sqrt{2}\, g\, q_o\, H_o}{\sqrt{\pi}(1+\lambda^2) u_b^3} \frac{w^2}{v}$.

the range of Kobus' experimental data.

An example of the agreement between predicted and experimental centerline velocities and plume widths as a function of elevation for a point source are shown in Figures 5a and 5b, respectively. The good agreement of velocity values in the near-source region manifests the difference between the formulation of the buoyancy flux term presented here and that of Kobus' analysis (7) which results in centerline velocities approaching zero in this region. The effect of the relative motion of the bubbles within the plume is demonstrated in Figure 5a. Curve 1 represents a solution which includes the bubble rise velocity u_b = 0.30m/s (representative of the size range of bubbles in most plumes, as discussed previously) and curve 2 a solution where bubble expansion is included but u_b neglected. The "slip" of the bubbles results in smaller plume velocities, and, of course, the most efficient plumes, from the water moving standpoint, are those with small bubbles which have small rise velocities.

Comparisons of velocity predictions and data for line sources are shown in Figures 6a and 6b. The experimental data for the line source were more scattered than for the point source as the air curtain apparently created seiching in the tank. The effects of varying the values of α and u_b in the model are shown by the three model predictions.

The comparisons of model predictions and Kobus' data for eight sets of point source data and three sets of line source data indicated that the model predicts air-bubble plume behavior well with the appropriate choices of u_b, λ, and α (9). The value of u_b = 0.30 m/s was found to be appropriate for Kobus' data and was consistent with rise velocity data in still water for bubbles 10^{-3}m to 10^{-2}m in diameter (2). The effect of variations in u_b on plume characteristics was relatively small as shown in Figure 6. The lateral spreading ratio value of λ = 0.2 was indicated with no significant variation in results with values of 0.1 and 0.3. The typical value of λ for single-phase buoyant plume systems is about 1.0 or slightly larger. For air-bubble systems the bubbles remain close to the plume centerline, and thus, relative to momentum, density deficiency is diffused laterally to a lesser degree. The entrainment coefficient, α, was found to vary with the rate of air discharge as shown in Figure 7. The value of α for a point source approaches 0.08 for large air flow rates. For single-phase simple plumes Rouse et al. (10) found α = 0.082. The entrainment process depends on the turbulent structure of the plume, and α is known to vary from 0.057 from point source momentum jets to 0.082 for point source buoyant plumes (11). Apparently, over the range of air discharge rates used in the experiments the mixing environment, and thus α, changed and approached that of a simple plume for large q_o. The data for the line source case are limited, but Figure 7 indicates values of α less than that of 0.16 reported by Lee and Emmons (12) for single-phase line source plumes. However, the data were for small range of air discharge and increased with increasing q_o. Further experimental results are needed to determine the value of α over a wider range of air discharges; however, Figure 7 can be used as a guide with the likely upper limits on α of 0.082 and 0.16 for point and line sources, respectively.

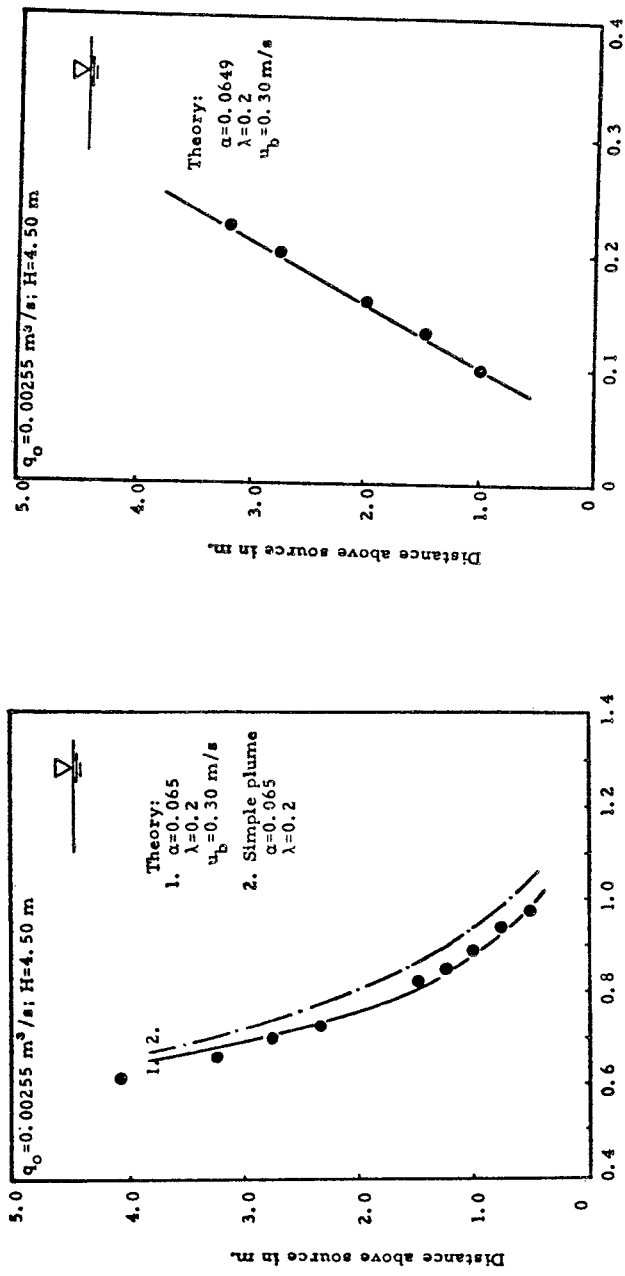

(a) Observed and predicted variation of centerline velocity with distance above the (real) source. Experimental data given by Kobus (1968).

(b) Observed and predicted rate of growth of the lateral velocity profile with the distance above the (real) source. Experimental data by Kobus (1968).

Figure 5

Figure 6

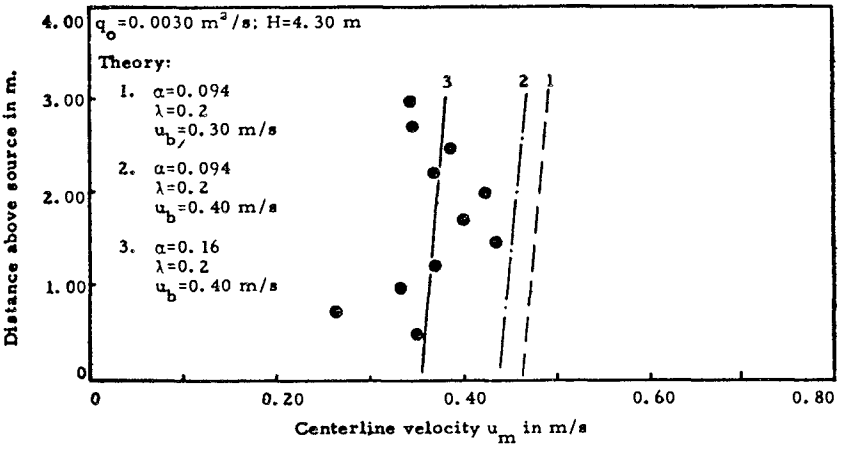

(a) Observed and predicted variation of centerline velocity with distance above the (real) source. Experimental data by Kobus (1968).

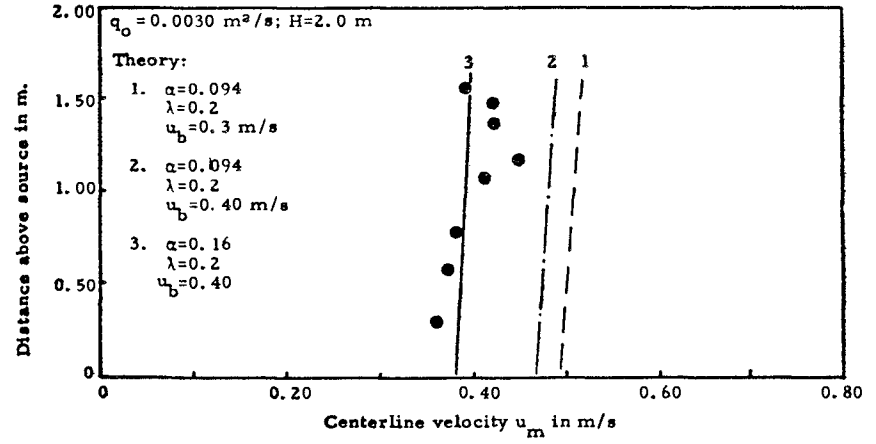

(b) Observed and predicted variation of centerline velocity with distance above the (real) source. Experimental data given by Kobus (1968).

Figure 7

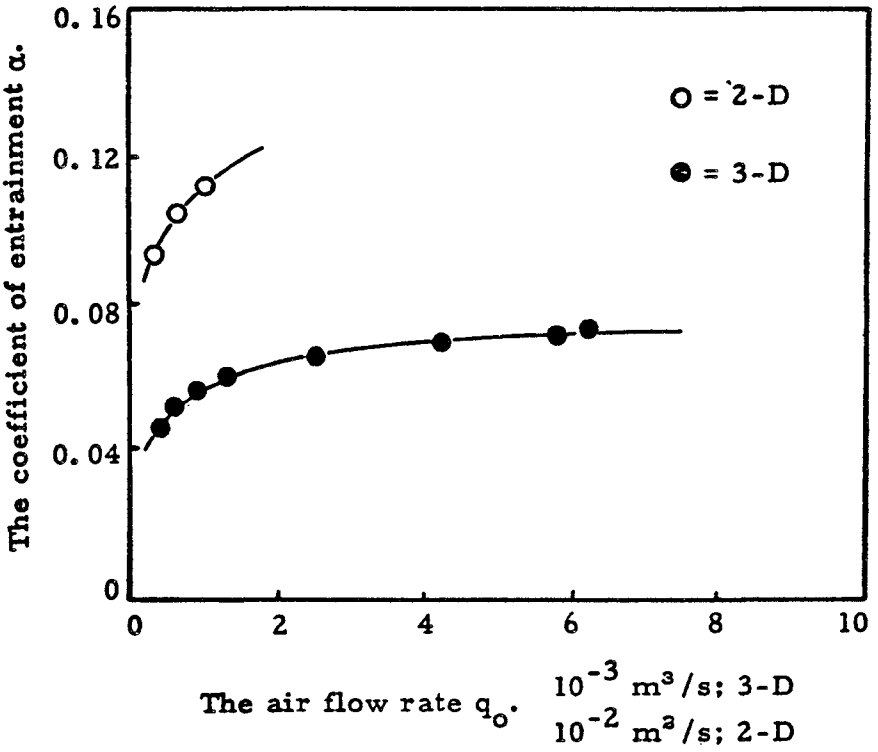

The coefficient of entrainment as a function of the air flow rate for two- and three-dimensional air-bubble plumes. Experimental data by Kobus (1968).

Conclusions

The analyses and generalized solutions for the cases of point source and line source air-bubble plumes provide predictions of the gross hydrodynamic features of such systems. These features are the velocity, width, and volume flux as a function of distance above the source. Comparisons of the analyses with large-scale experimental results indicated good agreement and yielded values for the lateral spreading ratio parameter and the entrainment coefficients. Application of the results requires that, in addition to the air discharge rate and description of the receiving water environment, only an estimate of the bubble rise velocity in still water be provided. Such estimates are available as a function of bubble size (2).

References

1. Davidson, J. F. and Schüler, B.O.G., "Bubble Formation at an Orifice in a Viscous Liquid," Trans. of the Inst. of Chem. Eng., Vol. 38, p. 144, 1960.

2. Haberman, W. L. and Morton, R. K., "An Experimental Study of Bubbles Moving in Liquids," ASCE Proc., Vol. 80, No. 387, Eng. Mech. Div., 1954.

3. Taylor, G. I., "The Action of a Surface Current Used as a Breakwater," Proc. Roy. Soc. A, Vol. 231, p. 466, 1955.

4. Bulson, P. S., "Bubble Breakwater with Intermittent Air Supply," Res. Rept. 9-2, Military Eng. Exper. Estab., Christchurch, Hampshire, England, 1962.

5. Bulson, P. S., "Large Scale Bubble Breakwater Experiments," Res. Rept. 9-3, Military Eng. Exper. Estab., Christchurch, Hampshire, England, 1962.

6. Sjöberg, A., "Strömnigshastigheter kring luft-bubbelrida i täthetshomogent och stillastående vatten (in Swedish)," Chalmers Inst. of Tech., Hydr. Div., Rept. No. 39, 1967.

7. Kobus, H. E., "Analysis of the Flow Induced by Air-Bubble Systems," Coastal Eng. Conf., London, Vol. II, p. 1016, 1968.

8. Morton, B. R. et al., "Turbulent Gravitational Convection from Maintained and Instantaneous Sources," Proc. Roy. Soc. A, Vol. 234, p.1, 1956.

9. Cederwall, K. and Ditmars, J. D., "Analysis of Air-Bubble Plumes," W. M. Keck Lab. of Hydraulics and Water Resources, Calif. Inst. of Tech., KH-R-24, 1970.

10. Rouse, H. et al., "Gravitational Convection from a Boundary Source," Tellus, Vol. 4, p. 201, 1952.

11. List, E. J. and Imberger, J., "Turbulent Entrainment in Buoyant Jets and Plumes," Proc. ASCE, Jour. Hydr. Div., Vol. 99, p. 1461, 1973.

12. Lee, S. L. and Emmons, H. W., "Study of Natural Convection Above a Line Fire," Jour. Fluid Mech., Vol. 11, p. 353, 1951.